

Spin-Spin Cross Sections of ^{27}Al and ^{93}Nb for Neutrons from 20 to 50 MeV

W. Heeringa, H. O. Klages, and Chr. Wöflf^(a)

*Institut für Kernphysik 1, Kernforschungszentrum Karlsruhe, Postfach 3640,
D-7500 Karlsruhe 1, West Germany*

R. W. Finlay

*John E. Edwards Accelerator Laboratory, Department of Physics and Astronomy,
Ohio University, Athens, Ohio 45701-2979*

(Received 13 February 1989)

Spin-spin cross sections of ^{27}Al and ^{93}Nb have been measured for neutrons between 20 and 50 MeV with high precision. Absolute size and energy dependence of the data agree well with existing predictions from folding-model calculations. The data can also be reproduced with phenomenological spin-spin potentials, but do not allow distinguishing between spherical and tensor interactions. The deduced spin-spin strengths are close to 1 MeV.

PACS numbers: 25.40.Dn, 24.10.Ht, 24.70.+s

In the past two decades there has been a steady interest in measuring the size of the nucleon-nucleus spin-spin interaction. The types of experiments carried out are transmission of polarized neutrons through polarized targets and depolarization measurements of polarized protons scattered from unpolarized targets. The aim of the experiments is to determine the direct spin-spin nucleon-nucleus interaction, derived from the spin-spin dependence in the nucleon-nucleon force. In the framework of the optical model, such an interaction can be expressed in terms of a spin-spin dependent potential like

$$U_{SS}(r) = -V_{SS}f_{SS}(r)\boldsymbol{\sigma}\cdot\mathbf{I}/I,$$

with V_{SS} and f_{SS} denoting the strength and the shape of the potential, \mathbf{I} the target spin, and $\boldsymbol{\sigma}$ the Pauli spin of the neutron. Besides a spherical interaction, tensor interactions may also be considered; the lowest order is

$$U_{ST}(r) = -V_{ST}f_{ST}(r)\frac{3(\boldsymbol{\sigma}\cdot\mathbf{r})(\mathbf{I}\cdot\mathbf{r})/r^2 - \boldsymbol{\sigma}\cdot\mathbf{I}}{2I}.$$

Depolarization can be originated by spin-spin interactions, by compound-nucleus scattering,¹ and by quadrupole spin flip.² The Erlangen group³ has measured the depolarization of protons in 10- and 11-MeV p - ^{27}Al scattering. After correction for compound-nucleus and quadrupole-spin-flip effects they obtained spin-spin potentials with strengths V_{SS} and V_{ST} both close to 2.5 MeV in the notation given above. At TRIUMF⁴ p - ^9Be depolarizations have been measured at 220 MeV, where compound-nucleus spin flip is negligible. A combined analysis in terms of quadrupole-spin-flip and spin-spin potentials yielded spherical and tensor spin-spin strengths slightly above 1 MeV in the above notation. Other depolarization results are less decisive.

In transmission experiments one measures the spin-spin cross section σ_{SS} defined as

$$\sigma_{SS} = (\sigma_p - \sigma_a)/2,$$

where σ_p and σ_a are the total cross sections for neutron and target spins parallel or antiparallel, respectively. The first transmission experiments have been usually carried out at low energy, a few MeV or below, and were largely consistent with zero. An exception are the data on ^{59}Co up to 3 MeV.^{5,6} Here a consistently negative σ_{SS} was found, which can be explained by effects due to compound-nucleus formation.^{7,8} For ^{59}Co also experiments at higher energies, up to 30 MeV, were carried out⁹ to determine the optical-model spin-spin potential. The data were no more than 1 standard deviation away from zero and set a limit of about 1 MeV to V_{SS} . Recently data on ^{27}Al were reported from Triangle Universities Nuclear Laboratory at four energies ranging from 5.2 to 16.5 MeV.¹⁰ From these data the authors deduce $V_{SS} = 0.75 \pm 0.44$ MeV, combined with an imaginary spin-spin strength $W_{SS} = -0.78 \pm 0.32$ MeV. The amount of data and the energy range are rather small, however, to test the energy dependence of σ_{SS} , as predicted by the optical model.

In this Letter we report σ_{SS} results on ^{27}Al and ^{93}Nb . The measurements were carried out with the polarized neutron beam of the facility POLKA¹¹ at the Karlsruhe cyclotron and the polarized-target facility KRYPTA.¹² The POLKA beam contains a continuous energy spectrum of polarized neutrons between approximately 20 and 50 MeV. They are produced with the $D(d,n)X$ reaction, using polarized deuterons from an atomic beam source, accelerated by the cyclotron to 52 MeV and directed onto a 1-cm-thick liquid- D_2 target. The neutron polarization is typically 50%, and the neutron energy is determined with time-of-flight techniques. Both neutron and target polarizations were oriented in the vertical direction in this experiment, and hence perpendicular to the beam. The size of the POLKA neutron beam was reduced to 20-mm diameter by means of an additional tungsten collimator of 40-cm length.

The neutron flux in front of the target was measured

by a 0.5-mm-thick NE 102A scintillator. It detected recoil protons, generated in a 7-mm-thick polyethylene converter positioned immediately in front of the scintillator. Protons from neutrons with energies below the useful energy range were stopped by a 0.5-mm aluminum absorber between the polyethylene and the scintillator. The scintillation light was reflected by a thin stainless-steel foil to a photomultiplier outside the neutron beam. The neutron flux behind the target was measured with a similar detector, having 13 mm of polyethylene and a 1-mm-thick NE 102A scintillator.

The targets were polarized in the KRYPTA cryostat, containing a ^3He - ^4He dilution refrigerator and a 9-T split coil magnet.¹² The ^{27}Al target had a quadratic cross section of $35 \times 35 \text{ mm}^2$, and the ^{93}Nb target had a circular cross section with a diameter of 30 mm. Both samples had thickness of 40 mm. Target temperatures were typically between 10 and 17 mK during the experiments, resulting in effective polarizations of 49% for ^{27}Al and of 53% for ^{93}Nb .

During the experiment the neutron polarization was switched every 4 sec to minimize systematic errors. Initially we switched between the up and down directions. However, due to an asymmetry of the rf transitions in the polarized deuteron source, the spin-up deuteron beam was contaminated with a varying amount of tensor polarization. Through the tensor analyzing power of the $D(d,n)X$ reactions¹³ this gave rise to a varying spin-up neutron flux. Because the tensor analyzing power is not constant over the neutron energy, the shape of the neutron flux spectrum was not constant in time, which is awkward for time-shift corrections. A similar problem was mentioned in Ref. 10. In order to avoid the inherent systematic uncertainties, we decided to carry out the final experiment by switching between zero and down polarization. The weak-field rf transition used for the down polarization has no measurable effect on the $m=0$ deuteron state; i.e., no tensor component occurs. The measurements were divided into runs of about 2-h length. The overall measuring time of both experiments was 300 h.

In the off-line analysis the data were divided in energy bins of 2 to 4 MeV in width (see Table I). Measurements with a warm (unpolarized) ^{93}Nb target were carried out to detect instrumental asymmetries. In a single energy bin these asymmetries did not exceed 3×10^{-4} . The average warm asymmetry was $\epsilon_w = (-1.2 \pm 0.5) \times 10^{-4}$. We did not correct for this small effect.

Our results of the cold (polarized) measurements are listed in Table I and shown in Fig. 1. One sees that the spin-spin cross sections are small, but that a part of the data clearly differs from zero. Moreover, both data sets exhibit a distinct energy trend. The curves in the figures are results of folding-model calculations by McAbee, Thompson, and Ohnishi.¹⁴ They find three spin-spin potentials contributing to σ_{SS} : the spherical one and two

TABLE I. Experimental results of the neutron spin-spin cross section for ^{27}Al and ^{93}Nb .

	E (MeV)	σ_{SS} (mb)	$\Delta\sigma_{SS}$ (mb)	
^{27}Al	22.0 ± 1.5	-7.0	7.3	
	25.0 ± 1.5	-6.6	5.2	
	27.5 ± 1.0	-7.0	5.8	
	30.0 ± 1.5	-0.9	5.1	
	33.0 ± 1.5	4.8	5.7	
	36.0 ± 1.5	0.6	6.5	
	40.0 ± 2.0	-4.1	7.0	
	50.0 ± 2.0	16.8	7.8	
^{93}Nb	19.0 ± 1.0	24.3	11.2	
	22.0 ± 1.5	13.1	4.8	
	25.0 ± 1.5	2.9	3.3	
	27.5 ± 1.0	-1.2	3.8	
	30.0 ± 1.5	-1.8	3.4	
	33.0 ± 1.5	-9.4	3.8	
	36.0 ± 1.5	-20.5	4.3	
	40.0 ± 2.0	-19.5	4.7	
		50.0 ± 2.0	-22.9	5.2

tensor potentials. There is a striking agreement between these predictions and our data, both in size and in energy dependence. For ^{93}Nb the prediction deviates at the highest energies. The data from Ref. 10 are also shown in Fig. 1.

We also compared our data with optical-model calculations using a version of the code SPINSOR, developed by Hussein and Sherif.¹⁵ The spin-spin cross sections are calculated in the distorted-wave Born approximation; hence the curves scale proportionally to V_{SS} or V_{ST} . Both spherical and first-order tensor spin-spin potentials were used with various radial shapes. Using the spherical potential good fits can be obtained for both nuclides only with a radial shape that peaks at about 70% of the nuclear radius. The tensor potential gives good fits for a surface-peaking radial shape. The results are shown in Fig. 2. The deduced parameters of the spin-spin potentials are listed in Table II. The errors were obtained by increasing $\chi^2(\text{min})$ by 1. The numbers have no absolute meaning because neither the relative strengths nor the radial shapes of the spherical and tensor potentials can be determined from these experiments. We show these calculations only to demonstrate that very nice fits can be obtained with spin-spin potentials of reasonable shape and strength. In the calculations the most recent optical-model parameter sets were used: for ^{27}Al , those from Martin,¹⁶ and for ^{93}Nb , from Walter and Guss.¹⁷

The analyses of our data show no indication for a possible imaginary spin-spin potential. As was pointed out in Ref. 10 the imaginary potential would generate a σ_{SS} which has a significantly different energy behavior as compared to σ_{SS} from a real potential. This would mean zero crossings at 20 and 60 MeV for ^{27}Al and at 20 and

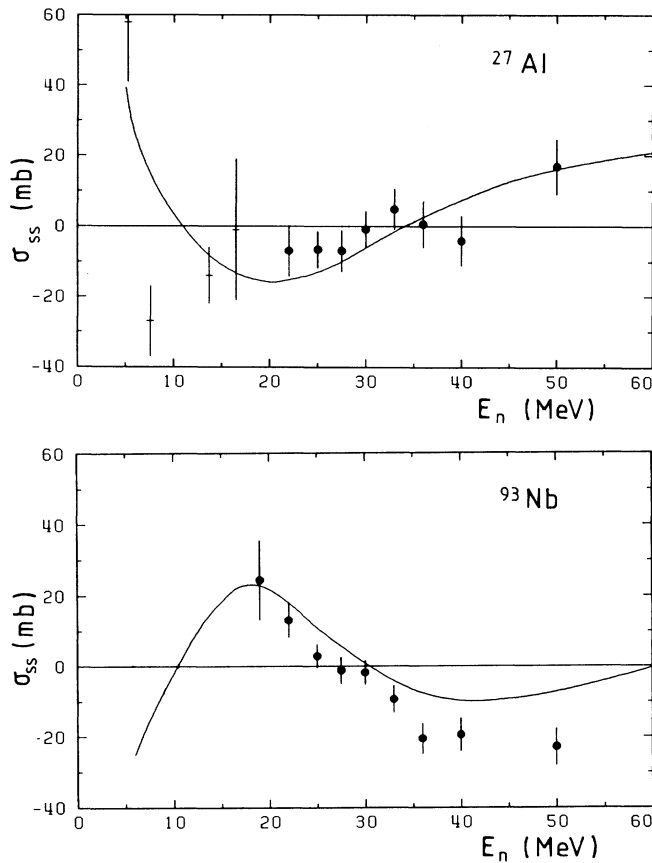


FIG. 1. Comparison of theoretical predictions with experimental spin-spin cross sections. Dots: this work; crosses: data from Ref. 10; the curves are predictions from Ref. 14.

45 MeV for ^{93}Nb . Our data nicely follow the energy trend given by the real spin-spin potential, and hence we do not confirm the rather large value of W_{SS} found by the authors of Ref. 10 for ^{27}Al at neutron energies from 5 to 16 MeV.

Contrary to the real nucleon-nucleon spin-spin potential, below the pion threshold an imaginary nucleon-nucleus spin-spin potential cannot be traced back to the spin dependence of the nucleon-nucleon interaction itself. Hence other mechanisms should be responsible for an eventual imaginary spin-spin interaction, such as spin-dependent compound-nucleus formation.^{7,8} It is doubtful, however, whether such a mechanism can be unambiguously translated into an imaginary spin-spin potential. Compound-nucleus formation produces steadily decreasing spin-spin effects due to the strongly increasing level densities, widths, and decay channels. An imaginary spin-spin potential yields an oscillatory σ_{SS} .

Spin-spin cross sections due to quadrupole deformation effects have been calculated recently by Hnizdo and Kemper¹⁸ for neutrons on ^{27}Al . Their calculations extend only up to 20 MeV, where our data begin. At 20

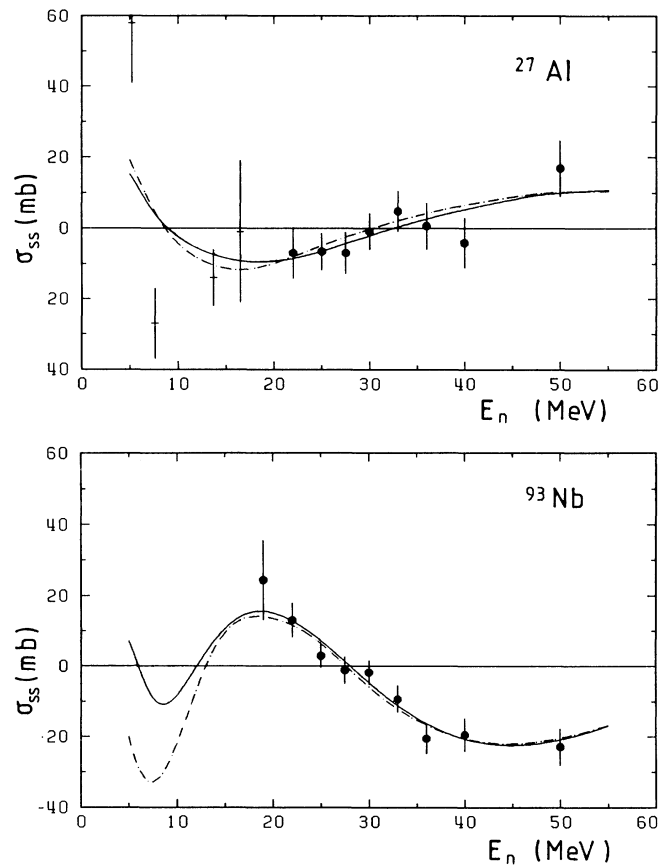


FIG. 2. Optical-model spin-spin cross sections fitted to our experimental results. Solid curves: spherical spin-spin potential; dash-dotted curves: first-order tensor spin-spin potential. The resulting spin-spin potential parameters are listed in Table II. Dots: this work; crosses: data from Ref. 10.

MeV they find $\sigma_{SS} = -8$ mb with a decreasing trend in absolute value. It was pointed out afterwards by Gould, Roberson, and Thompson,¹⁹ that the quadrupole moment employed by Hnizdo and Kemper is a factor of 2 too high. This reduces the result at 20 MeV to $\sigma_{SS} = -4$ mb. Our data from 20 to 40 MeV are essentially consistent with this value. It would be interesting to see quadrupole-deformation-effect calculations for ^{27}Al

TABLE II. Spin-spin potential parameters found in fitting our new data separately by a spherical and by a first-order tensor spin-spin potentials. The last column gives the values of χ^2/D per data point.

	V_{SS} (keV)	V_{ST} (keV)	a_{SS}	r_{SS}	χ^2/D
^{27}Al	850 ± 350		0.65	0.89	0.45
^{93}Nb	1090 ± 230		0.40	0.85	0.55
^{27}Al		-2250 ± 980	1.21	1.07	0.54
^{93}Nb		-2160 ± 250	0.69	1.22	0.59

above 20 MeV. The effects are expected to be negligible for ^{93}Nb , due to its small quadrupole deformation.

We conclude that our σ_{SS} results are the first with sufficient accuracy over a wide enough energy range to allow a meaningful comparison with theoretical models. The data agree well with folding-model predictions of McAbee, Thompson, and Ohnishi.¹⁴ A phenomenological description using well-determined values for the remaining optical-model parameters yields very good descriptions of the data with real spherical spin-spin potentials close to 1 MeV.

We thank D. Reppenhagen for help in the early stages of the data analysis and for running the deuteron polarimeter. The help of P. Doll, V. Eberhard, T. D. Ford, and H. Krupp in the data taking is gratefully acknowledged. We thank the crews of the polarized deuteron source and the cyclotron for providing the polarized deuteron beam. We also thank the authors of Ref. 14 for allowing us to show their results prior to publication.

^(a)Now with Dornier, Friedrichshafen, West Germany.

¹W. J. Thompson, Phys. Lett. **62B**, 245 (1976).

²J. S. Blair, M. P. Baker, and H. S. Sherif, Phys. Lett. **60B**, 25 (1975).

³R. Schmitt *et al.*, J. Phys. Soc. Jpn., Suppl. **55**, 578 (1986).

⁴G. Roy *et al.*, Nucl. Phys. **A442**, 686 (1985).

⁵T. R. Fisher, H. A. Grench, D. C. Healey, J. McCarthy, D.

Parks, and R. Whitney, Nucl. Phys. **A179**, 241 (1972).

⁶W. Heeringa and H. Postma, Phys. Lett. **61B**, 350 (1976).

⁷W. J. Thompson, Phys. Lett. **65B**, 309 (1976).

⁸W. Heeringa and H. Postma, Phys. Rev. C **27**, 2012 (1983).

⁹W. Heeringa, H. Postma, H. Dobiash, R. Fischer, H. O. Klages, R. Maschuw, and B. Zeitnitz, Phys. Rev. C **16**, 1389 (1977).

¹⁰C. R. Gould, D. G. Haase, L. W. Seagondollar, J. P. Soderstrum, K. E. Nash, M. B. Schneider, and N. R. Roberson, Phys. Rev. Lett. **57**, 2371 (1986).

¹¹H. O. Klages *et al.*, Nucl. Instrum. Methods, Phys. Res. **219**, 26 (1984).

¹²R. Aures, W. Heeringa, H. O. Klages, R. Maschuw, F. K. Schmidt, and B. Zeitnitz, Nucl. Instrum. Methods, Phys. Res. **224**, 347 (1984).

¹³J. E. Simmons, W. E. Broste, G. P. Lawrence, J. L. McKibben, and G. G. Ohlsen, Phys. Rev. Lett. **27**, 113 (1971).

¹⁴T. L. McAbee, W. J. Thompson, and H. Ohnishi (to be published); T. L. McAbee, Ph.D. thesis, University of North Carolina, Chapel Hill, 1986, University Microfilms (unpublished).

¹⁵A. H. Hussein and H. S. Sherif, Phys. Rev. C **8**, 518 (1973).

¹⁶Ph. Martin, Nucl. Phys. **A466**, 119 (1987).

¹⁷R. L. Walter and P. P. Guss, Radiat. Eff. **95**, 73 (1986).

¹⁸V. Hnizdo and K. W. Kemper, Phys. Rev. Lett. **59**, 1892 (1987).

¹⁹C. R. Gould, N. R. Roberson, and W. J. Thompson, Phys. Rev. Lett. **60**, 2335 (1988).